Computers and Concrete, Vol. 4, No. 2 (2007) 101-117
DOI: http://dx.doi.org/10.12989/cac.2007.4.2.101

3D material model for nonlinear basic creep of concrete

Jörg Bockhold†

ZERNA INGENIEURE, Engineering Consultants, Industriestraβe 27, 44892 Bochum, Germany

(Received September 1, 2005, Accepted February 5, 2007)

Abstract. A new model predicting the nonlinear basic creep behaviour of concrete structures subjected to high multi-axial stresses is proposed. It combines a model based on the thermodynamic framework of the elasto-plastic continuum damage theory for time-independent material behaviour and a rheological model describing phenomenologically the long-term delayed deformation. Strength increase due to ageing is regarded. The general 3D solution for the creep theory is derived from a rate-type form of the uniaxial formulation by the assumption of associated creep flow and a theorem of energy equivalence. The model is able to reproduce linear primary creep as well as secondary and tertiary creep stages under high compressive stresses. For concrete in tension a simple viscoelastic formulation is applied. The material law is then incorporated into a finite element solution procedure for analysis of reinforced concrete structures. Numerical examples of uniaxial creep tests and concrete members show excellent agreement with experimental results.

Keywords: concrete; creep; damage; plasticity; finite-element analysis.

1. Introduction

The serviceability and long-term performance of concrete structures is strongly influenced by the time-dependent behaviour of the material. Quasi-brittle, cementitious materials such as concrete exhibit creep deformations, that can be significantly larger than the time-invariant, instantaneous ones, due to their viscoelastic properties. The interaction of the evolution of creep strains and microcracking may cause in addition a considerable reduction of the structural lifetime, which may even lead to a delayed structural collapse.

The incorporation of the most important physical influences on the origin of creep into a numerical prediction model is still a subject of extensive scientific studies. In the past decades, intense efforts have been made to formulate theories for the approximation of creep strains in concrete structures. Since early constitutive creep models based on empirical functions and derived from experimental observations, major success has been made in defining more sophisticated theories (Bažant and Wu 1974, Bažant and Chern 1984). The transition from the definition of phenomenological models to physically based creep models enabled to take moisture diffusion and its influence on long-term deformation into account (Bažant and Najjar 1971 Wittmann and Roelfstra 1980). This led to a deeply improved understanding of the physical influences on creep. The developed theories have been further supported by consideration of ageing of the material as a consequence of cement hydration, characterised by a volume growth of the hydration products (Bažant and Prasannan 1989). With these achievements, models have been established to simulate

† E-mail: jbo@zerna.eu

close-to-reality a significant decreasing creep evolution with the age of material increasing. With the work of Bažant, *et al*. (1997), which unified the theories of concrete solidification and long-term creep, the development of linear ageing viscoelastic creep models has become essentially accomplished.

However, if ultimate limit state analyses of concrete structures have to be performed, the interaction between concrete microcracking and nonlinear creep at high compressive stresses seems to be still one of the most important problems, that have to be examined (van Zijl, de Borst and Rots 2001). Only a few material models can be found, in which nonlinear basic creep evolution under high compressive stresses is considered. Frequently used nonlinear material models, that couple creep and damage evolution, are based on the Solidification Theory or its extension the Microprestress Solidification Theory (Mazzotti and Savoia 2003, Cervera, *et al.* 1999, Ozbolt and Reinhardt 2001). It has been proven, that these models provide a suitable basis for simulation of nonlinear creep effects. Nevertheless, they consider material nonlinearities by an artificial extension of the underlying formulation, such as empirical damage or creep acceleration functions. A combination of arbitrary 3D stress-strain-states with nonlinear, divergent creep strain evolution and time-invariant elasto-plastic-damage behaviour is not considered in these theories.

Therefore in this paper a recently proposed time-invariant material model for concrete is extended to account for long-term nonlinear basic creep to analyse the influence of delayed deformations on the long-term behaviour and structural safety of reinforced concrete structures. The theoretical framework of this model is based on the multisurface elasto-plastic continuum damage theory. Irreversible plastic strains as well as damage, which is phenomenologically seen as a reduction of the elastic stiffness, is accounted for. Long-term creep evolution is decribed with help of a rheological model in analogy to well-known viscoelastic theories, but built up of nonlinear spring-dashpot-systems. This enables not only to simulate primary creep, but also both secondary and tertiary creep stages, where micro-cracks develop, coalesce and where finally a macro-crack leads to local material instability. The differential equation for the creep strains gained from the rheological model is reformulated in a rate-type form to consider the time-dependent ageing of the material. This contributes to a realistic estimation of the long-term response of concrete structures. This uniaxial creep model is extended to three-dimensional stress conditions by means of an associative evolution law just like in well-known plasticity models. The relationship between the general 3D state and the equivalent uniaxial state is established with help of an energy dissipation assumption. Numerical examples show, that this creep law is able to directly fit generally known experimental benchmark tests.

2. Time-invariant material model

The total material formulation for concrete is separated into two parts: A time-invariant material model (short-term model), which predicts the time-invariant mechanical response of the material, and a constitutive creep law (long-term model), which describes time-dependent nonlinear basic creep deformations. In this section, only the basic formulations for the short-term model, which are important for extension onto creep, are presented briefly. A more detailed description can be found in Krätzig and Pölling (2004) and Bockhold, *et al*. (2003). The advantage of this material formulation is that it unifies all major deterioration phenomena of concrete, namely damage and plasticity, with help of only a few material parameters.

The fundamental basis of the presented concept is the stress-based elasto-plastic continuum damage theory (Govindjee, *et al.* 1995). This theory represents a convenient framework for the numerical simulation of the nonlinear material behaviour of ductile-brittle materials such as concrete, which exhibit residual plastic deformations as well as damage due to micro-cracking. The basic idea is, that the evolution of damage on the micromechanical level is phenomenologically considered as the reduction of the macroscopic modulus of elasticity. Therefore the plastic strain tensor $\varepsilon^{\mathrm{pl}}$, the damage compliance tensor of fourth order $\mathbb{D}^{\mathrm{da}}$ and the scalar hardening variable q are selected as thermodynamical internal variables. The corresponding stress-strain relation reads:

$$\boldsymbol{\sigma} = (\mathbb{D}^{0} + \mathbb{D}^{\mathrm{da}})^{-1} : (\boldsymbol{\varepsilon} - \boldsymbol{\varepsilon}^{\mathrm{pl}}) \tag{1}$$

The domain of admissible stresses E is defined in the space of associated variables through a flow/damage potential ϕ:

$$E = \{(\boldsymbol{\sigma},\ \alpha(q)) | \phi(\boldsymbol{\sigma} \otimes \boldsymbol{\sigma},\ \alpha(q)) \leq 0\} \tag{2}$$

where $\alpha(q)$ defines the hardening/softening function. If the material is unloaded, irreversible strains as well as a reduced elastic stiffness can be observed. In order to distinguish plastic from damaging strains, the total inelastic strain tensor is seperated into a plastic and damaging part with help of the scalar variable β, where $0 \leq \beta \leq 1$, as originally proposed in Meschke, *et al.* (1998). Assuming associated plastic/damaging flow, one may write:

$$\dot{\boldsymbol{\varepsilon}}^{\mathrm{pl}} = (1-\beta)\frac{\partial \phi}{\partial \boldsymbol{\sigma}}\dot{\lambda} \quad \text{and} \quad \dot{\boldsymbol{\varepsilon}}^{\mathrm{da}} = \beta \frac{\partial \phi}{\partial \boldsymbol{\sigma}}\dot{\lambda} \tag{3}$$

In Eq. (3) $\dot{\lambda}$ represents the consistency parameter, which defines the amount of plastic/damaging flow, while the derivative $\partial\phi/\partial\boldsymbol{\sigma}$ gives the direction of it in stress space. The formulation for the evolution of the internal variable $\alpha(q)$ is derived from the principle of maximum inelastic dissipation:

$$\dot{\alpha} = \frac{\partial \phi}{\partial \alpha}\frac{\partial \alpha}{\partial q}\dot{\lambda} \tag{4}$$

With these definitions the fundamental aspects of the time-invariant material formulation are presented. For the extension with regard to long-term creep deformations the further description is distinguished between concrete under compressive and under tensile loading.

2.1. Concrete under compression

To describe the behaviour of concrete under compression, a yield/damage potential of Drucker-Prager type is used, which is especially applicable for concrete under dominant biaxial stress states. It is defined through the first invariant I_1 of the stress tensor, the second invariant J_2 of the stress deviator $\mathbf{s}$, a parameter μ, which controls the influence of the hydrostatic stresses on damage or yield, and the hardening/softening function $\alpha_c(q_c)$ as follows

$$\phi_c(\boldsymbol{\sigma}, \alpha_c) = \frac{1}{\frac{1}{\sqrt{3}} - \mu}[\mu I_1 + \sqrt{J_2}] - \alpha_c(q_c) \tag{5}$$

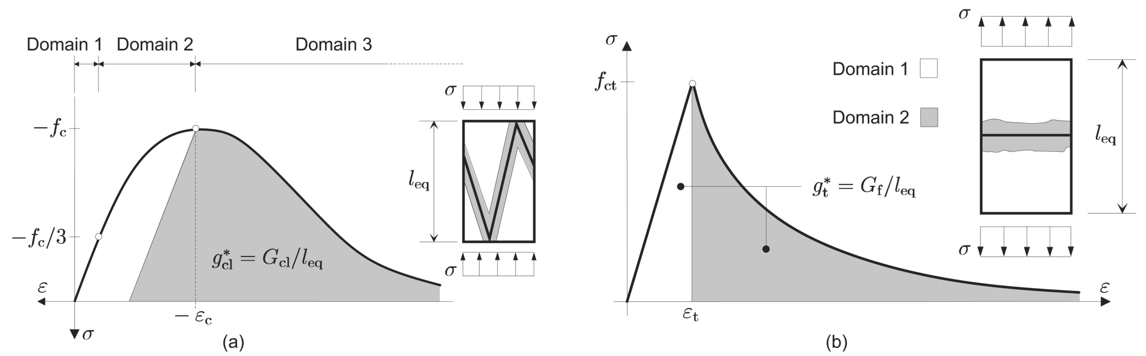

Fig. 1 Uniaxial stress-strain relation used for concrete under (a) compression and (b) tension

where the subscript ‘c’ refers to concrete under compression. The hardening/softening behaviour of concrete in compression is controlled by defining the function $\alpha_c(q_c)$ by means of the uniaxial stress-strain relation given in the Model Code (CEB/FIP 1991):

$$\alpha_c(q_c) = \overline{\sigma}(\varepsilon(q_c)) . \tag{6}$$

The relation is separated into three different branches as graphically shown in Fig. 1(a): A linear-elastic, a strain hardening and a strain softening branch. The latter is characterised by damage localization in narrow fracture zones and by formation of macro-cracks. To overcome a mesh dependence of the solution, the fracture energy concept is adopted here (Bažant and Oh 1983). It defines the softening branch in dependence on the fracture energy G_{cl} and on the characteristic length l_{eq} of the finite element.

2.2. Concrete under tension

For concrete under tensile loading it is assumed, that in each of the main stress directions, characterised by the three eigenvalues of the stress tensor and its corresponding eigenbases, a crack may develop completely autonomous. For simplicity, plastic strains are in addition neglected (β=1) and nonlinear hardening is not regarded (see Fig. 1(b)). Tensile failure is described with a damage potential of Rankine type:

$$\phi_{t,(i)}(\boldsymbol{\sigma}, \boldsymbol{\alpha}_t) = \xi^{(i)} - f_{ct} \le 0, \qquad i = 1,2,3 \tag{7}$$

where $\xi^{(i)}$ represents the i-th eigenvalue of $\boldsymbol{\xi}=\boldsymbol{\sigma}-\boldsymbol{\alpha}_t$, f_{ct} defines the tensile strength of concrete and the subscript ‘t’ refers to concrete under tension. The internal history variable $\boldsymbol{\alpha}_t$ denotes the back-stress tensor. The derivatives of the potential with respect to $\boldsymbol{\sigma}$ and $\boldsymbol{\alpha}_t$ yield the eigenvalue bases of $\boldsymbol{\xi}$:

$$\frac{\partial \phi_{t,(i)}}{\partial \boldsymbol{\sigma}} = \mathbf{M}_{\xi}^{(i)}, \quad \frac{\partial \phi_{t,(i)}}{\partial \boldsymbol{\alpha}_t} = -\mathbf{M}_{\xi}^{(i)} . \tag{8}$$

Finally, applying the normality rule

$$\dot{\boldsymbol{\varepsilon}}_t^{da} = \mathbb{D}_t^{da} : \boldsymbol{\sigma} = \sum_{i=1}^{3} \dot{\lambda}_{t,(i)} \frac{\partial \phi_{t,(i)}}{\partial \boldsymbol{\sigma}} = \sum_{i=1}^{3} \dot{\lambda}_{t,(i)} \mathbf{M}_{\xi}^{(i)} \tag{9}$$

Table 1 Material parameters of the time-invariant model

f_c	Compressive strength	E_c	Young's modulus
f_{ct}	Tensile strength	ν_c	Poisson's ratio
ε_c	Crushing strain	G_f	Fracture energy
G_{c1}	Crushing energy	b	Damage parameter
μ	Biaxial failure parameter		

and the anisotropic damage rule from (Govindjee, *et al.* 1995)

$$\mathbb{D}_t^{da} = \sum_{i=1}^{3} \dot{\lambda}_{t,(i)} \frac{\mathbf{M}_\xi^{(i)} \otimes \mathbf{M}_\xi^{(i)}}{\mathbf{M}_\xi^{(i)} : \boldsymbol{\sigma}} \tag{10}$$

the evolution laws for the main variables have been derived. The formulation of the kinematic softening rule is described in detail in Krätzig and Pölling (2004).

Damage localization is again considered by means of the fracture energy G_f and the characteristic length l_{eq} of the respective finite element as indicated in Fig. 1(b).

The time-invariant material model for concrete under compression and tension is unified in the framework of the multi-surface material theory (de Borst and Gutiérrez 1999, Hofstetter and Mang 1995). It contains only 9 material parameters, which are summarised in Table 1. The key advantage of this model is, that it combines all major deterioration phenomena of concrete, namely irreversible plastic strains and stiffness degradation or damage due to micro-cracking. It is furthermore able to reproduce the cyclic deformation behaviour of the material with help of a minimum number of well-defined, experimentally identifiable material parameters. The material formulation is therefore very well applicable for close-to-practice numerical simulations of complex concrete structures (Petryna and Krätzig 2005). The extension of this model to account for long-term nonlinear creep will be shown in the following section.

3. Nonlinear 3D basic creep model

Concrete under high sustained compressive stresses exhibits creep deformations, that can be significantly larger than the deformations resulting from time-invariant, instantaneous loadings (Mazzotti and Savoia 2002). While in the domain of service loads, which can be characterised by stress levels up to one third of the compressive strength, the assumption of a linear relation between stresses and creep strains is reasonable, a nonlinear increase of creep strains is observed, if this domain is exceeded. For stresses above approximately 80% of f_c two additional major aspects emerge, as visualised in Fig. 2: The domain of primary creep, usually observed in low-stress creep tests, turns over into a domain of secondary creep, which is characterised by constant creep strain increase. This deformation behaviour is additionally accompanied by evolution and coalescence of micro-cracks (Meyers, *et al.* 1969). If the stress level stays constant, or even does not decrease, a tertiary creep domain is initiated. At this point the creep evolution becomes strongly nonlinear, leading to divergent deformations due to extensive micro-cracking and finally to local material failure. This behaviour is counteracted by a gradual increase of the concrete stiffness and strenght as a result of cement hydration.

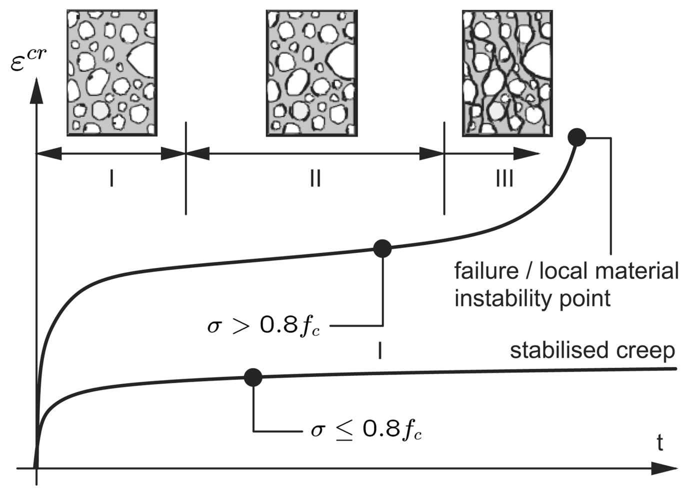

Fig. 2 Qualitative creep behaviour of concrete under low and high stresses

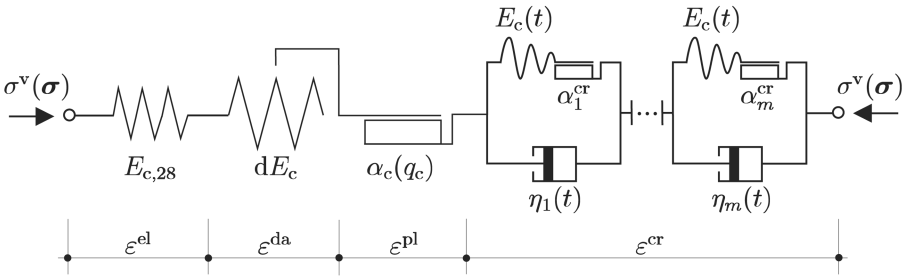

Fig. 3 Rheological model combining short-and long-term strains

A general 3D constitutive creep model is presented in the following part of this paper, which is able to reproduce numerically not only nonlinear creep deformations of concrete under sustained high loads but also long-term evolution of damage and its coupling with instantaneous, short-term deteriorations. The creep model is based on a rate-type formulation and takes time-dependent ageing into account. Through the coupling with the previously presented time-invariant elasto-plastic continuum damage model, the material description represents general constitutive law, that is able to reproduce nonlinear creep as well as stress relaxation responses originating from arbitrary un- and reloading cycles.

The extension of the presented time-invariant model for long-term nonlinear creep deformations is performed by using a rheological chain, as presented in Fig. 3. This chain represents the mechanical interpretation of the general 3D materials response on a given sudden or sustained loading. The short-term model is defined through the individual fractions of initial elastic strains $\varepsilon^{\mathrm{el}}$, damage strains $\varepsilon^{\mathrm{da}}$ and plastic strains $\varepsilon^{\mathrm{pl}}$. The long-term behaviour is governed using a series of spring-dashpot chains (creep chains), in analogy to the classical theory of viscoelasticity (Tschoegl 1989). According to this and assuming small strain measures, the (linearised) strain tensor can be decomposed into a time-invariant and a time-dependent part

$$\boldsymbol{\varepsilon} = \boldsymbol{\varepsilon}^{\mathrm{el}} + \boldsymbol{\varepsilon}^{\mathrm{da}} + \boldsymbol{\varepsilon}^{\mathrm{pl}} + \boldsymbol{\varepsilon}^{\mathrm{cr}} \tag{11}$$

where $\boldsymbol{\varepsilon}^{cr}$ defines the creep strain tensor. Since the rheological chain represents an uniaxial analogy to the general 3D case, a transformation rule from uni-to multi-axial stress and strain states has to be found. In accordance with classical plasticity theories (Simo and Hughes 1998, Simo, *et al.* 1988) the assumption of associated plastic flow is extended here to account for creep strains. The underlying assumption is, that creep and plastic strains can be regarded as completely equivalent, since they originate from the same load in different time scales. This leads to the following evolution equation (Pfister and Stangenberg 2005):

$$\dot{\boldsymbol{\varepsilon}}^{cr} = \dot{\lambda}^{cr}\frac{\partial \phi}{\partial \boldsymbol{\sigma}} \tag{12}$$

where $\dot{\lambda}^{cr}$ defines the creep consistency parameter. The evolution law is derived from the assumption of equivalence of uniaxial and 3D energy dissipation. It is proposed, that the energy dissipated by a given stress state and by the appendant strain increment is equal to that energy, which is dissipated by an equivalent uniaxial stress, that is derived from the 3D stress state with help of the flow potential, and the accordant uniaxial creep strain increment. The corresponding mathematical relation reads:

$$\boldsymbol{\sigma} : \dot{\boldsymbol{\varepsilon}}^{cr} = \sigma^{eq}(\boldsymbol{\sigma}) \cdot \dot{\varepsilon}^{cr} \tag{13}$$

A given stress tensor $\boldsymbol{\sigma}$ is accordingly transformed into the equivalent uniaxial stress $\sigma^{eq}(\boldsymbol{\sigma})$. Substituting Eq. (12) into Eq. (13) yields the evolution law for the creep consistency parameter:

$$\dot{\lambda}^{cr} = \frac{\sigma^{eq}(\boldsymbol{\sigma}) \cdot \dot{\varepsilon}^{cr}}{\boldsymbol{\sigma} : \dfrac{\partial \phi}{\partial \boldsymbol{\sigma}}} \tag{14}$$

where $\dot{\varepsilon}^{cr}$ is the unixial creep rate derived from the mechanical model. Finally, with the creep consistency parameter known, the increment of the creep strain tensor is calculated with help of Eq. (12).

The transformation rule Eq. (14) represents a very convenient and applicable way to conclude from a simple uniaxial stress state to a more complicated multi-axial one. The creep model has to be validated therefore only at uniaxial creep tests. Once this has been done, it can be applied to the numerical simulation of arbitrary complex concrete structures.

For concrete under compression and under tension a different creep behaviour can be observed. Under compressive loadings, as mentioned before, a strong nonlinear increase of delayed strains up to material failure can be detected. However, if the material is loaded under sustained tensile stresses, the relation between stresses and creep strains can be regarded as linear viscoelastic (Karihaloo and Santhikumar 1998). Therefore the following formulation is used for concrete under compression only. For concrete under tension, a simple viscoelastic model is used, which is not discussed more closely in this paper.

The creep strains for concrete under compression are calculated from the rheological chain indicated in Fig. 3. The key idea is, that the implied material response of the uniaxial spring and dashpot due to an imposed stress is directly verified by experimental observations. The obtained results for the creep strains show good agreement with experimental data. They are gained without need of extensive curve fitting procedures or artificial extensions.

As pointed out before, the stress-strain relation of concrete under a sustained load is limited by the long-term compressive strength $f_{c,T} \approx 0.8 f_c$. Therefore it is assumed, that the spring of the

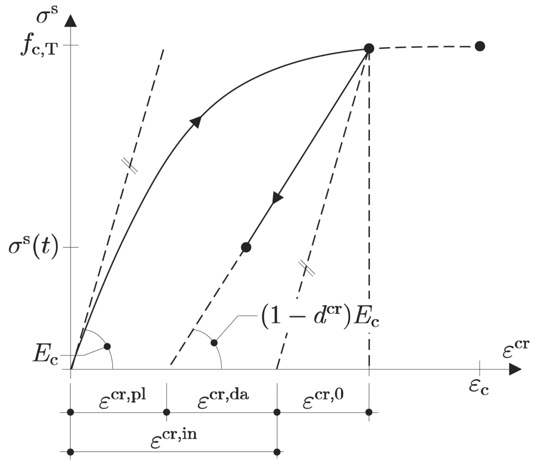

Fig. 4 Stress-strain relation of the spring of the creep model

rheological chain is controlled by a nonlinear stress-strain relation taken from the Model Code (CEB/FIP 1991) now restricted by $f_{c,T}$:

$$\sigma^s = \frac{E_c \dfrac{\varepsilon^{cr}}{f_{c,T}} + \left(\dfrac{\varepsilon^{cr}}{\varepsilon_c}\right)^2}{1 - \left(E_c \dfrac{\varepsilon_c}{f_{c,T}} - 2\right)\left(\dfrac{\varepsilon^{cr}}{\varepsilon_c}\right)} f_{c,T} \,. \tag{15}$$

Fig. 4 illustrates the stress-strain relation of the spring. To pay attention to ageing of concrete, all material parameters in this relation are time-dependent. Irreversible plastic creep strains $\varepsilon^{cr,pl}$ are considered by introducing an additional plastic slip element, which is controlled by the stress-equivalent internal variable α^{cr}. If the plastic flow condition $\phi^{cr} = |\sigma^s| - \alpha^{cr} < 0$ is violated, plastic/ damaging flow takes place and the internal variable is set to $\alpha^{cr} = |\sigma^s|$. Otherwise the spring is unloaded. In this case linear unloading is assumed, where, in analogy to the time-invariant material model, a scalar variable b decomposes inelastic creep strains into plastic and damaging ones:

$$\varepsilon^{cr,pl} = b \cdot \varepsilon^{cr,in}, \text{ and: } \varepsilon^{cr,da} = (1-b) \cdot \varepsilon^{cr,in} \,. \tag{16}$$

Following the work of Meschke (1998), as a result of strength and stiffness increase additional temporal irreversible creep strains $\varepsilon^{cr,t}$ occur. Under the assumption, that the modulus of elasticity $E_c(t)$ is a finite, nonzero value, which approaches for $t \to \infty$ the value E_c^∞, the rate of $\varepsilon^{cr,t}$ can be calculated as

$$\dot{\varepsilon}^{cr,t} = \kappa(\dot{\varepsilon}^{cr} - \dot{\varepsilon}^{cr,pl}) \quad \text{with} \quad \kappa = 1 - \frac{E_c(t)}{E_c^\infty} \,. \tag{17}$$

The dashpot of the creep chain in Fig. 3 is governed through a linear relation between the stresses σ^d and the creep strain rates $\dot{\varepsilon}^{cr}$, depending on the viscosity η of the material. In this paper, the viscosity is modified in that way, that the special time-dependent deformation behaviour of concrete can be suitably reproduced. The first modification accounts for the special shape of creep curves. It can be deduced from experimental observations, that the viscosity η of concrete may be defined as a variable, which increases monotonically with time. Hence, if t_0 is the age of the material at loading, for $(t - t_0) \rightarrow 0$ the viscosity also tends to zero.

The second modification incorporates the stress-dependency of η. It follows from experimental observations of concrete specimen under high sustained loads, that not only the magnitude of creep strains of a higher loaded specimen is larger, than that of a lower loaded one, also the creep strains develop faster. This phenomenon, which can be interpreted physically as a process of material consolidation, is considered here by using a stress-dependent formulation for η.

With these assumptions the viscosity of the dashpot is defined in the following form:

$$\eta(\sigma^{\mathrm{eq}}(\boldsymbol{\sigma}), t, t_0) = E_{\mathrm{c},0}\, \mathcal{T} \left(\frac{t-t_0}{\mathcal{T}}\right)^{0.5} \left(1 - \frac{\sigma^{\mathrm{eq}}(\boldsymbol{\sigma})}{f_{\mathrm{c},0}}\right)^2 \tag{18}$$

where the subscript '0' refers to the age of the material at loading and $\mathcal{T}$ represents the retardation time, defining the velocity of stress exhaustion inside the dashpot. The equivalent stress $\sigma^{\mathrm{eq}}(\sigma)$ is determined form the Drucker-Prager potential as

$$\sigma^{\mathrm{eq}}(\boldsymbol{\sigma}) = \frac{1}{\frac{1}{\sqrt{3}} - \mu}[\mu I_1 + \sqrt{J_2}]\,. \tag{19}$$

Then the relation between stresses and strain rates inside the dashpot is defined through

$$\sigma^d = \eta(\sigma^{\mathrm{eq}}(\boldsymbol{\sigma}), t, t_0) \cdot \dot{\varepsilon}^{\mathrm{cr}}\,. \tag{20}$$

The relations for the stresses in Eq. (15) and Eq. (20) obviously violate the second law of thermodynamics, due to the fact, that they incorporate ageing constituents (Bažant and Chern 1984). To overcome the ill-posedness of the mathematical problem the stresses are expanded into a Taylor-series of first order in time. Therefore in accordance to Bažant's exponential algorithm (Bažant and Wu 1974), it is assumed, that the stress varies linearly over a given time interval $[t_n; t_{n+1}]$, where $t_{n+1} = t_n + \Delta t$ and Δt represents the incremental time step:

$$\sigma_{n+1} = \sigma_n + \Delta t\, \dot{\sigma}_{n+1}\,. \tag{21}$$

Under the assumption that f_{c}, E_{c} and ε_{c} are constant during a sufficiently small time-increment and that the tangent modulus C_{T} is approximately equal to that of the last time step and in analogy to the stress formulation of the dashpot the stress rate of the spring reads

$$\dot{\sigma}^{\mathrm{s}}_{n+1} = \frac{\mathrm{d}\sigma^{\mathrm{s}}}{\mathrm{d}\varepsilon^{\mathrm{cr}}}\frac{\mathrm{d}\varepsilon^{\mathrm{cr}}}{\mathrm{d}t} \approx C_{\mathrm{T},n}\dot{\varepsilon}^{\mathrm{cr}}_{n+1}\,. \tag{22}$$

In this equation the tangent modulus is defined as:

$$C_{\mathrm{T},n} = \frac{\left(\frac{E_{\mathrm{c}}}{f_{\mathrm{c}}} + 2\frac{\varepsilon^{\mathrm{cr}}_n}{\varepsilon^2_{\mathrm{c}}}\right) f_{\mathrm{c}}}{1 - \left(\frac{E_{\mathrm{c}}\varepsilon_{\mathrm{c}}}{f_{\mathrm{c}}} - 2\right)\frac{\varepsilon^{\mathrm{cr}}_n}{\varepsilon_{\mathrm{c}}}} + \frac{\left(\frac{\varepsilon^{\mathrm{cr}}_n E_{\mathrm{c}}}{f_{\mathrm{c}}} + \left(\frac{\varepsilon^{\mathrm{cr}}_n}{\varepsilon_{\mathrm{c}}}\right)^2\right) f_{\mathrm{c}}\left(\frac{E_{\mathrm{c}}\varepsilon_{\mathrm{c}}}{f_{\mathrm{c}}} - 2\right)}{\left(1 - \left(\frac{E_{\mathrm{c}}\varepsilon_{\mathrm{c}}}{f_{\mathrm{c}}} - 2\right)\frac{\varepsilon^{\mathrm{cr}}_n}{\varepsilon_{\mathrm{c}}}\right)^2 \varepsilon_c}\,. \tag{23}$$

The stress rate of the dashpot takes the well-known form for ageing materials:

$$\dot{\sigma}^{\mathrm{d}}_{n+1} = \frac{\mathrm{d}(\eta_{n+1}+\dot{\varepsilon}^{\mathrm{cr}}_{n+1})}{\mathrm{d}t} = \dot{\eta}_{n+1}\dot{\varepsilon}^{\mathrm{cr}}_{n+1}+\dot{\eta}_{n+1}\ddot{\varepsilon}^{\mathrm{cr}}_{n+1} \tag{24}$$

with

$$\dot{\eta}(\sigma^{\mathrm{eq}}(\boldsymbol{\sigma}),t,t_0) = \frac{E_{\mathrm{c},0}}{2}\left(\frac{t-t_0}{\mathcal{T}}\right)^{-0.5}\left(1-\frac{\sigma^{\mathrm{eq}}(\boldsymbol{\sigma})}{f_{\mathrm{c},0}}\right)^2. \tag{25}$$

Defining stress equilibrium at the rheological chain gives the differential equation for nonlinear basic creep of ageing concrete:

$$\sigma^{\mathrm{eq}}_{n+1}(\bullet) = \sigma^{\mathrm{s}}_{n+1}+\sigma^{d}_{n+1} = \sigma^{\mathrm{s}}_{n}+C_{\mathrm{T},n}\Delta t\dot{\varepsilon}^{\mathrm{cr}}_{n+1}+\sigma^{\mathrm{d}}_{n}+\Delta t(\dot{\eta}_{n+1}+\dot{\varepsilon}^{\mathrm{cr}}_{n+1}+\eta_{n+1}+\ddot{\varepsilon}^{\mathrm{cr}}_{n+1}) \tag{26}$$

which has to be solved regarding the creep strain $\varepsilon^{\mathrm{cr}}_{n+1}$. This can be done with well-known implicit time integration procedures, e.g., with the NEWMARK-scheme (Newmark 1959). This delivers the unknown values $\varepsilon^{\mathrm{cr}}$, $\dot{\varepsilon}^{\mathrm{cr}}$ and $\ddot{\varepsilon}^{\mathrm{cr}}$ at t_{n+1}.

In the case of unloading ($\phi^{\mathrm{cr}} < 0$), the spring follows a linear-elastic stress path. Then also the temporal irreversible and the plastic creep strains as well as the scalar creep-damage variabel d^{cr} have to be known. These are calculated as follows: With the *Backward-Euler*-integration

$$(\bullet)_{n+1} = (\bullet)_n+\Delta(\bullet)_{n+1} \quad \text{and} \quad \frac{\mathrm{d}(\bullet)}{\mathrm{d}t}\approx\frac{\Delta(\bullet)}{\Delta t} \tag{27}$$

where (•) represents an arbitrary variable, Eq. (17) is rewritten in an incremental form:

$$\Delta\varepsilon^{\mathrm{cr,t}}_{n+1} = \kappa(\Delta\varepsilon^{\mathrm{cr}}_{n+1}-\Delta\varepsilon^{\mathrm{cr,pl}}_{n+1}) \tag{28}$$

The linear-elastic stress-strain relation is given in accordance to Meschke (1998) as

$$\sigma^{\mathrm{s}} = (1-d^{\mathrm{cr}})E^{\infty}_{c}(\varepsilon^{\mathrm{cr}}-\varepsilon^{\mathrm{cr,pl}}-\varepsilon^{\mathrm{cr,t}}) \tag{29}$$

From this and keeping Eq. (16) in mind, the actual plastic creep strain increment is defined through:

$$\Delta\varepsilon^{\mathrm{cr,pl}}_{n+1} = b\cdot\varepsilon^{\mathrm{cr,in}}_{n+1} = b\left(\varepsilon^{\mathrm{cr}}_{n+1}-\frac{\sigma^{\mathrm{s}}_{n+1}}{E^{\infty}_{c}}-\varepsilon^{\mathrm{cr},t}_{n+1}\right) \tag{30}$$

With Eq. (28) and Eq. (30) the incremental change of $\varepsilon^{\mathrm{cr,pl}}$ is obtained as

$$\Delta\varepsilon^{\mathrm{cr,pl}}_{n+1} = b\left[\varepsilon^{\mathrm{cr}}_{n}+\kappa\cdot\Delta\varepsilon^{\mathrm{cr}}_{n+1}-\frac{\sigma^{\mathrm{s}}_{n+1}}{E^{\infty}_{c}}-\varepsilon^{\mathrm{cr,t}}_{n}\right]\cdot[1-b(1-\kappa)]^{-1} \tag{31}$$

Finally, the creep-damage variable can be defined in the following way:

$$d^{\mathrm{cr}}_{n+1} = 1-\frac{\sigma^{\mathrm{s}}_{n+1}}{E^{\infty}_{\mathrm{c}}(\varepsilon^{\mathrm{cr}}_{n+1}-\varepsilon^{\mathrm{cr,pl}}_{n+1}-\varepsilon^{\mathrm{cr,\,t}}_{n+1})} \tag{32}$$

The solution of this incremental procedure depends on the applied stress $\boldsymbol{\sigma}$. Of course, in the context of strain driven finite element calculations, the creep strains contribute to the total amount of strains and therefore influence the actual level of stresses in the respective Gauss point. Since a new creep strain increment leads to an unbalancing of the internal stress-strain equilibrium condition, an alternating iterative updating algorithm of stresses, plastic and creep strains is used. It is based on the classical stress-based multi-surface return mapping algorithm. For details see e.g., Simo, *et al*. (1988), Ortiz and Martin (1989), Simo and Hughes (1998).

4. Numerical examples

The following numerical examples are presented to illustrate the accuracy of the proposed combined elasto-plastic continuum damage model for concrete under short-and long-term loading. At first some features of the model with regard to nonlinearities and age of the concrete are discussed. After that a series of creep tests is simulated numerically to underline the model qualities on material point level. Finally, creep buckling of a reinforced concrete column is analysed.

4.1. Model features

The qualitative prediction behaviour of the creep model and the influence of the time-dependent ageing of the concrete on the long-term deformation is analysed in Fig. 5. The numerical simulation is carried out with three creep chains with retardation times of $\mathcal{T} = 1 \cdot 10^3$, $1 \cdot 10^4$ and $\mathcal{T} = 1 \cdot 10^5$ and time step sizes of $\Delta t = 0.01$[d]. Ageing of concrete is considered by means of a time-dependent function for the compressive strength in accordance to (Nechvatal 1996):

$$f_c(t) = 10.99 + 7.4 \cdot \ln(t)\ [\mathrm{MN/m^2}] \tag{33}$$

while for the modulus of elasticity E_c and the crushing strain ε_c of the creep chain the following relations originally proposed by Nechvatal (1996) and de Schutter and Taerwe (1996) are used:

$$E_c[f_c(t)] = 5606.9\sqrt{f_c(t)} \tag{34}$$

$$\varepsilon_c[f_c(t)] = 0.00044 \cdot \sqrt[3]{f_c(t)} + \frac{0.0021}{\sqrt{f_c(t)}}\,. \tag{35}$$

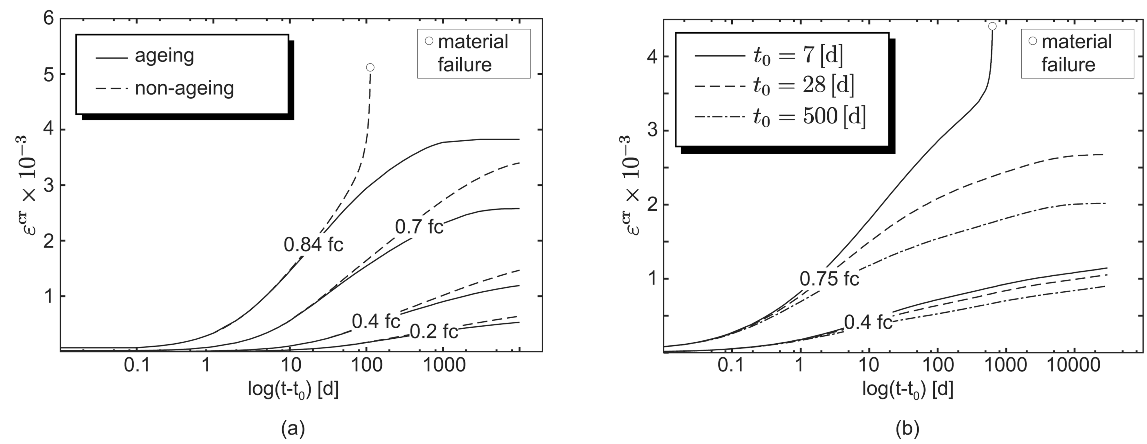

Fig. 5 Analysis of the influence of ageing on concrete creep

From Fig. 5 it can be seen, that the developed model is generally able to simulate nonlinear basic creep. A non-proportional increase of creep strains under rising stresses as well as secondary and tertiary creep domains under stresses above the creep resistance $f_{c,T}$ is predicted. In Fig. 5(a) the sensitivity of creep with respect to cement hydration in combination with the stress level is analysed. It can be seen, that after approximately 100 days of sustained loading differences in the calculated creep curves of the ageing and non-ageing material dramatically increase. The magnitude of differences strongly depends on the load level. Under high stresses, the numerical simulations yield a completely different solution, if ageing of the material is neglected.

The role of time-dependent material parameters is also analysed in Fig. 5(b), which shows calculated creep curves depending on the age t_0 of the material at loading. Again, a big difference between the predicted curves is given for high loads. In the domain of service loads stress and strength variation with time seems to be less important, while at high stresses the age of the concrete defines, whether the material fails or not.

4.2. Creep experiments

We now analyse the prediction quality of the developed long-term material model by means of experimental results taken from Roll (1964) and Nechvatal (1996). The numerical simulation is carried with the material parameters given in Table 2. The number of creep chains as well as the retardation times of each chain have been found by validation at the creep test with the lowest applied stress. The numerical simulation at higher stresses is then performed with the same

Table 2 Material parameters used for creep simulations on material point level

	$f_{c,28}$ [MN/m^2]	$\mathcal{T}_1$ [d]	$\mathcal{T}_2$ [d]	$\mathcal{T}_3$ [d]	$\mathcal{T}_4$ [d]	$\mathcal{T}_5$ [d]
Roll (1964)	42.0	$5 \cdot 10^2$	$1 \cdot 10^3$	$5 \cdot 10^3$	$1 \cdot 10^4$	$5 \cdot 10^4$
Nechvatal (1996)	35.6	$1 \cdot 10^2$	$1 \cdot 10^4$	$1 \cdot 10^5$	–	–

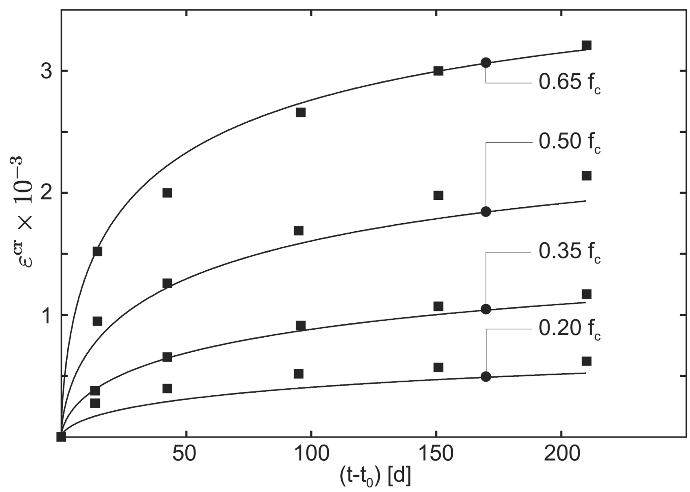

Fig. 6 Calculated creep strains at different load levels (—) in comparison to experimental results obtained by Roll (1964) (■)

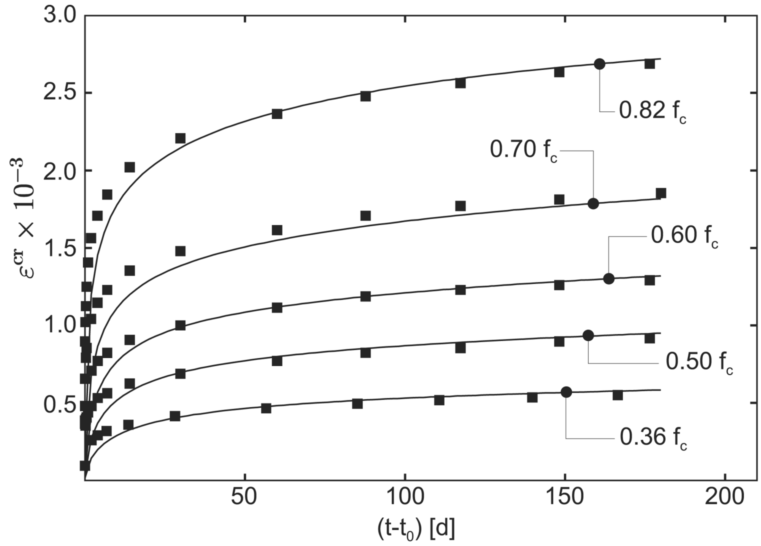

Fig. 7 Calculated creep strains at different load levels (—) in comparison to experimental results obtained by (Nechvatal 1996) (■)

parameters without any further adaption.

A comparison of calculated and experimental creep strains in Fig. 6 and Fig. 7 shows a satisfying agreement for low, medium and high stresses. Not only the final creep value is well predicted in the numerical simulation, also the evolution of creep strains in time is reproduced accurately. The developed material theory is obviously able to model long-term creep of concrete quantitively and qualitatively close-to-reality.

4.3. RC column under sustained loading

Finally, the material model is used in the context of the nonlinear finite element method to study the lifetime performance of an eccentrically loaded reinforced concrete column under sustained loading in comparison to experimental results. For the numerical simulation a 3D continuum-based finite shell element is used (Krätzig and Jun 2003). The element formulation is based on multi-layer kinematics as shown in Fig. 8. Steel reinforcement is modelled as uniaxial layer with smeared material properties and elasto-plastic material behaviour, which takes isotropic and kinematic hardening into account.

Fig. 9 provides the geometry and the load arrangement of the column and the material parameters used in the numerical simulation. The column is discretised with 12 finite elements. To study the short-and long-term performance of the structure several load scenarios are carried out according to an experimental program of three identical columns documented in Espion (1993). In Fig. 10 the numerical solution is compared to the experimental data. The first column has been initially loaded up until failure. From Fig. 10 (left) it can bee seen, that the maximum load P = 444 [kN] is suitably approximated in the simulation. The column fails due to buckling as a result of progressive tensile cracking and stiffness reduction. The second column is loaded initially up to P = 250 [kN]. The load is kept constant for 200 days and afterwards again increased until structural failure. For creep

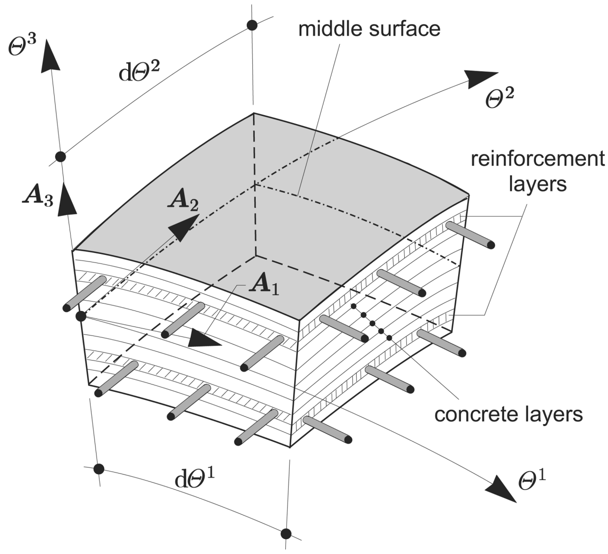

Fig. 8 3D continuum-based shell element with multi-layer kinematics

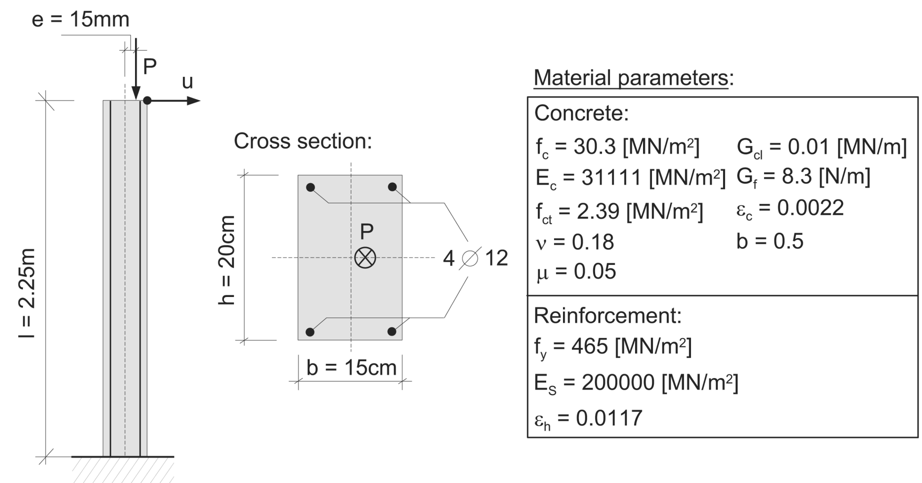

Fig. 9 Geometry of the RC column and material parameters used for the numerical analysis

simulation four creep chains with retardation times of $\mathcal{T} = 1 \cdot 10^2$, $5 \cdot 10^2$, $\mathcal{T} = 1 \cdot 10^3$ and $\mathcal{T} = 1 \cdot 10^4$ [d] are used. The calculated load-deflection curve in Fig. 10 (left) shows good agreement with the experimental data. Obviously, the creep deformations lead to a reduced maximum carrying capacity. The maximum load is reduced to 345 [kN], which is 78% of the initial value. The lifetime performance under creep deformation is analysed by means of a third experiment. For this, the column is subjected to a sustained load of $P = 280$ [kN], which is only 12% higher than the previous creep load. Fig. 10 (right) gives the corresponding time-deflection curves for both, creep experiments and numerical simulation. Now the higher loaded column is subjected to a time-dependent stability failure due to progressive creep deformations. The reason for this is the interaction between geometrical and physical nonlinearities. The creep strains lead to a new

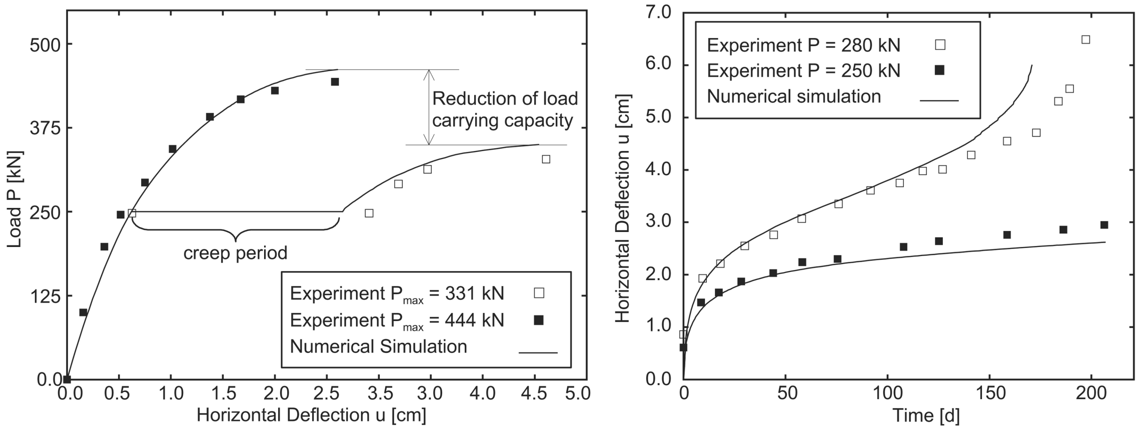

Fig. 10 Short-and long-term deflection of the RC column under sustained load

deformation state with changed stresses and progressive micro-cracking. If a critical load factor is exceeded the deformations increase until equilibrium between internal and external forces is lost. A good agreement between the numerical and the experimental solution can be observed.

This example shows, that creep deformations may lead to a reduced carrying capacity and to a reduced lifetime of reinforced concrete structures. In some cases it may even lead to time-dependent stability failure. This structural behaviour can be well reproduced with help of the presented material model.

5. Conclusions

This paper proposes a new 3D material model to simulate the lifetime behaviour of reinforced concrete structures under nonlinear basic creep deformations. It consists of a time-invariant material model for concrete, which is based on the elasto-plastic continuum damage theory, and a time-dependent rheological model, which incorporates explicitly the nonlinear relations between stresses and creep strains and stresses and creep strain rates. Ageing of the material is considered with help of time-dependent material parameters. The material model is able to cover the whole range of creep strains from low to high stress levels. The interaction between geometrical and physical nonlinearities in reinforced conrete structures is analysed in the framework of the finite element method with help of a 3D continuum-based shell element. Numerical examples underline the efficiency of the proposed model and emphasise the effect of creep on the lifetime performance of a column under eccentrical loading.

Acknowledgements

Financial support of the German Research Foundation (DFG) within Project A5 of the Collaborative Research Center SFB 398 at the Ruhr-University Bochum is gratefully acknowledged.

References

Bažant, Z. P. and Chern, J. C. (1984), "Rate-type concrete creep law with reduced time", *J. Eng. Mech.,* **110**, 329-340.

Bažant, Z. P., Hauggaard, A. B., Baweja, S. and Ulm, F. J. (1997), "Microprestress-solidification theory for concrete creep. I: Aging and drying effects. II: Algorithm and verification", *J. Eng. Mech.,* **123**(11), 1188-1201.

Bažant, Z. P. and Najjar, L. J. (1971), "Drying of concrete as a nonlinear diffusion problem", *Cement Concrete Res.,* **1**, 461-473.

Bažant, Z. P. and Oh, B. (1983), "Crack band theory for fracture concrete". *J. Eng. Mech.,* **16**(93), 155-177.

Bažant, Z. P. and Prasannan, S. (1989), "Solidification theory for concrete creep. I: Formulation. II: Verification and application", *J. Eng. Mech.,* **115**, 1691-1725.

Bažant, Z. P. and Wu, S. T. (1974), "Rate-type creep law of ageing concrete based on maxwell chain", *Mater. Struct.,* **7**, 45-60.

Bockhold, J., Krätzig, W. B., Pölling, R. and Petryna, Y. S. (2003), "Material model for concrete under monotonic loading and creep", In N. Bićanić, R. de Borst, H. Mang, and G. Meschke (Eds.), *Computational Modelling of Concrete Structures*, 401-410. Balkema.

CEB/FIP (1991), CEB-FIP Model Code 1990 (Design Code).

Cervera, M., Oliver, J. and Prato, T. (1999), "Thermo-chemo-mechanical model for concrete. I: Hydration and aging. II: Damage and creep. *J. Eng. Mech.* **125**(9), 1018-1039.

de Borst, R. and Gutiérrez, M. A. (1999), "A unified framework for concrete damage and fracture models including size effects", *Int. J. Fracture,* **95**, 261-277.

de Schutter, G. and Taerwe, L. (1996), "Degree of hydration-based description of mechanical roperties of early age concrete", *Mater. Struct.,* **29**, 335-344.

Espion, B. (1993), "Benchmark examples for creep and shrinkage analysis computer programs", In Z.P. Bazant and I. Carol (Eds.), *Creep and Shrinkage of Concrete*, 877-888. E & FN Spon, London.

Govindjee, S., Kay, G. J. and Simo, J. C. (1995), "Anisotropic modelling and numerical simulation of brittle damage in concrete", *Int. J. Numer. Methods Eng.,* **38**, 3611-3633.

Hofstetter, G. and Mang, H. A. (1995), *Computational mechanics of reinforced concrete structures*. Grundlagen und Fortschritte der Ingenieurwissenschaften. Braunschweig: Vieweg & Sohn.

Karihaloo, B. L. and Santhikumar, S. (1998), "Time-dependent behaviour of cracked and ageing concrete", *Proceeding of EURO-C* 1998 (139-166).

Krätzig, W. B. and Pölling, R. (2004), "An elasto-plastic damage model for reinforced concrete with minimum number of material parameters", *Comput. Struct.,* **82**, 1201-1215.

Krätzig, W. B. and Jun, D. (2003), "On 'best' shell models - From classical shells, degenerated and multi-layer concepts to 3D", *Archive of Applied Mechanics,* **73**, 1-25.

Mazzotti, C. and Savoia, M. (2002), "Nonlinear creep, possion's ratio and creep-damage interaction of concrete in compression", *ACI Mater. J.,* **99**(5), 450-457.

Mazzotti, C. and Savoia, M. (2003), "Nonlinear creep damage model for concrete under uniaxial compression", *J. Eng. Mech.,* **129**(9), 1065-1075.

Meschke, G. (1998), "Consideration of aging of shotcrete in the context of a 3D viscoplastic material model", *Int. J. Numer. Methods Eng.,* **39**, 3123-3143.

Meschke, G., Lackner, R. and Mang, H. A. (1998), "An anisotropic elastoplastic-damage model for plain concrete", *Int. J. Numer. Methods Eng.,* **42**, 703-727.

Meyers, B. L., Slate, F. O. and Winter, G. (1969), "Relationship between time-dependent deformation and micro-cracking of plane concrete", *ACI J.,* **66**, 60-69.

Nechvatal, D. (1996), *Normalbeton unter hohen Dauerlasten bei verhindertem Feuchteaustausch*. Ph. D. thesis, Lehrstuhl für Massivbau, Technische Universität München. In German.

Newmark, N. M. (1959), "A method of computation for structural dynamics", *J. Eng. Mech. Div. (ASCE),* **3**, 67-94.

Ortiz, M. and Martin, J. B. (1989), "Symmetry-preserving return mapping algorithms and incrementally extremal paths: A unification of concepts", *Int. J. Numer. Methods Eng.,* **28**, 1839-1853.

Ozbolt, J. and Reinhardt, H. W. (2001), "Creep-cracking interaction of concrete-threedimensional finite element model", In F.-J. Ulm, Z. P. Bažant, and F.H. Wittmann (Eds.), *Creep, Shrinkage and Durability Mechanics of Concrete and other Quasi-Brittle Materials*, 221-228. Elsevier Science Ltd.

Petryna, Y. S. and Krätzig, W. B. (2005), "Computational framework for long-term reliability analyis of RC structures", *Comp. Methods Appl. Mech. Eng.,* **194**, 1619-1639.

Pfister, T. and Stangenberg, F. (2005), "Fatigue lifetime assessment of RC members", In G. Augusti, G. I. Schuëller, and M. Ciampoli (Eds.), *Safety and Reliability of Engineering Systems and Structures*, Rome, Italy, 19-23 June 2005, CD-ROM. ICOSSAR '05: Mill-press.

Roll, R. (1964), "Long time creep-recovery of highly stressed concrete cylinders", In *ACI SP-9 Symposium on creep*, 115-128. Portland Cement Association.

Simo, J. C. and Hughes, T. J. R. (1998), *Computational inelasticity*. New York, Berlin, Heidelberg: Springer Verlag.

Simo, J. C., Kennedy, J. G. and Govindjee, S. (1988), "Non-smooth multisurface plasticity and viscoplasticity. Loading/Unloading conditions and numerical algorithms", *Int. J. Numer. Methods Eng.* **26**, 2161-2185.

Tschoegl, N. W. (1989). *The Phenomenological Theory of Linear Viscoelastic Behavior*. Springer-Verlag.

van Zijl, G. P. A. G., de Borst, R. and Rots, J. G. (2001), "A numerical model for the time-dependent cracking of cementitious materials". *Int. J. Numer. Methods Eng.,* **52**, 637-654.

Wittmann, F. H. and Roelfstra, P. E. (1980) "Total deformation of loaded drying concrete", *Cement Concrete Res.,* **10**, 601-610.

NB